Density Functional Study of Some Germylene Insertion Reactions

Ming-Der Su* and San-Yan Chu*

*Contribution from the Department of Chemistry, National Tsing Hua University,
Hsinchu 30043, Taiwan, ROC*

Received October 28, 1998. Revised Manuscript Received February 16, 1999

Abstract: Complete geometry optimizations were carried out using density functional theory to study potential energy surfaces for the insertion of germylene into C−H bonds of methane. The GeXY + CH$_4$ (GeXY = GeH$_2$, Ge=CH$_2$, GeH(CH$_3$), Ge(CH$_3$)$_2$, GeHF, GeF$_2$, GeHCl, GeCl$_2$, GeHBr, and GeBr$_2$) systems are the subject of the present study. All the stationary points were determined at the B3LYP/6-311G* level of theory. Our theoretical findings suggest that the computed structures of germylenes are in good agreement with the available experimental results, with the bond lengths and angles in agreement to within 0.04 Å and 1.0°, respectively. A configuration mixing model based on the theory of Pross and Shaik has been used to develop an explanation for the barrier height as well as the reaction enthalpy. Our theoretical findings suggest that the singlet−triplet splitting ($\Delta E_{st} = E_{triplet} - E_{singlet}$) of the GeXY species can be used as a guide to predict its activity for insertion reactions. Thus, the major conclusion that can be drawn from this work is as follows: the more strongly π-accepting, the bulkier, or the more electropositive the substituents, the smaller the ΔE_{st} of GeXY, the lower the activation energy, and the larger the exothermicity for the insertion of GeXY into saturated C−H bonds. In other words, it is the electronic factors, rather than steric factors, that play a decisive role in determining the chemical reactivity of the germylene species.

I. Introduction

Germylene (GeXY) is an intriguing chemical species which is isoelectronic with carbene, silylene, and oxygen. Although intuitively its chemical behavior is expected to be similar to that of its isoelectronic homologues, its chemistry has hitherto been far less well explored. Thus far, only one example of insertion of germylene into a C−H bond has been described.[1−3] The chemical reactivity of GeH$_2$ in its ground state is still comparatively unknown. Indeed, it is astonishing how little is known about the reactivity of germylenes, considering the importance of germanium hydrides in semiconductor processing[4−7] and the extensive research activity on the corresponding carbene and silylene species.[8] Further, systematic investigations of the chemistry of germylenes would not only be academically rewarding but practically important,[9,10] primarily because of the role they may play in a variety of semiconductor growth processes.

Carbenes undergo characteristic chemical reactions such as insertion into a single bond, addition to a double bond, dimerization, and intramolecular rearrangement.[8] The chemical behavior of carbenes is strongly dependent upon their spin multiplicity.[8] Triplet carbenes react by two-step radical processes, whereas singlet carbenes can undergo single-step bond

insertions. It is therefore reasonable to expect that the reactivity of substituted germylenes will also be influenced by their spin multiplicity. As will be shown below, the germylenes investigated in this study all have singlet ground states and are therefore expected to undergo insertion reactions. In contrast to the wealth of experimental and theoretical information on carbene and silylene insertion reactions,[8] relatively little is known concerning the mechanisms of germylene insertions. To examine the reactivity of the parent germylene, GeH$_2$, as well as numerous substituted germylenes, we have undertaken a systematic investigation of the insertion reactions of various germylene derivatives into C−H bonds (eq 1) using density functional theory (DFT).

$$\text{GeXY} + \text{H−CH}_3 \rightarrow \text{Ge(X)(Y)(H)(CH}_3\text{)} \qquad (1)$$

We have considered the reaction paths of a model insertion of GeXY into the C−H bond of methane, where GeXY = GeH$_2$,

(1) Lange, L.; Meyer, B.; DuMont, W.-W. *J. Organomet. Chem.* **1987**, *329*, C17.

(2) Neumann, W. P. *Chem. Rev.* **1991**, *91*, 311.

(3) (a) Lukevics, E.; Gar, T.; Ignatovich, L.; Mironov, B. In *Biological Activity of Germanium*, Zinatne, Riga: 1990. (b) Lukevics, E.; Ignatovich, L. In *Frontiers of Organogermanium−Tin−Lead Chemistry*; Latvian Institute: Riga, 1993. (c) Patai, S. In *the Chemistry of Organic Germanium, Tin and Lead Compounds*; Wiley: New York, 1995.

(4) Motooka, T.; Greene, J. E. *J. Appl. Phys.* **1986**, *59*, 2015.

(5) Du, W.; Keeling, L. A.; Greenlief, C. M. *J. Vac. Sci. Technol.* **1994**, *A12*, 2281.

(6) Isobe, C.; Cho, H.; Crowell, J. E. *Surf. Sci.* **1993**, *295*, 117.

(7) Lu, G.; Crowell, J. E. *J. Chem. Phys.* **1993**, *98*, 3415.

(8) For reviews, see: (a) Hine, J. In *Divalent Carbon*; Academic Press: New York, 1964. (b) Krimes, W. In *Carbene Chemistry*, 1st ed.; Academic Press: New York, 1964; Chapter 1. (c) Bethell, D. *Adv. Phys. Org. Chem.* **1969**, *7*, 153−209. (d) Moss, R. A. In *Selective Organic Transformations*; Thyagarajan, B. S., Ed.; Wiley: New York, 1970; pp 35−88. (e) Krimes, W. In *Carbene Chemistry*, 2nd ed.; Academic Press: New York, 1971; Chapter 8. (f) Moss, R. A.; Jones, M., Jr. In *Carbenes*; Wiley: New York, 1973; Vol. 1. (g) Jones, M., Jr.; Moss, R. A. In *Carbenes*; Wiley: New York, 1975; Vol. 2. (h) Moss, R. A.; Jones, M., Jr. In *Reactive Intermediates*; Wiley: New York, 1978; Vol. 1. (i) Moss, R. A.; Jones, M., Jr. In *Reactive Intermediates*; Wiley: New York, 1981; Vol. 2, Chapter 3. (j) Moss, R. A.; Jones, M., Jr. In *Reactive Intermediates*; Wiley: New York, 1985; Vol. 3, Chapter 3. (k) Abramovitch, R. A. In *Reactive Intermediates*; Plenum: New York, 1980; Vol. 1. (l) Platz, M. S. In *Kinetics And Spectroscopy of Carbenes And Biradicals*; Plenum: New York, 1990. (m) DeMore, W. B.; Benson, S. W. *Adv. Photochem.* **1964**, *2*, 219−261. (n) Tomioka, H. *Res. Chem. Intermed.* **1994**, *20*, 605−634. (o) Closs, G. L. In *Topics in Stereochemistry*; Eliel, E. L., Allinger, N. L., Eds.; Interscience: New York, 1968; Vol. 3, pp 193−235.

(9) Jutzi, P.; Schmidt, H.; Neumann, B.; Stammler, H.-G. *Organometallics* **1996**, *15*, 741.

(10) Lei, D.; Lee, M. E.; Gaspar, P. P. *Tetrahedron* **1997**, *53*, 10179.

Ge=CH$_2$, GeH(CH$_3$), Ge(CH$_3$)$_2$, GeHF, GeF$_2$, GeHCl, GeCl$_2$, GeHBr, and GeBr$_2$. These molecules have been chosen as model systems for insertions into CH$_4$ because most of their spectroscopic and electronic properties have been studied experimentally in some detail. For instance, the various spectra for GeH$_2$,[11-15] Ge=CH$_2$,[16] GeF$_2$,[17,18] GeHCl,[19,20] GeCl$_2$,[21,22] GeHBr,[20,23] and GeBr$_2$[24] have been reported in the literature. In the present study, we compute the chemical reactivities of all 10 of these molecules. We use DFT to explore the effect of different substitutions on the insertion of germylene into methane molecule. The purpose of the present DFT mechanical study is to locate the transition state for reaction 1, to carry out a vibrational analylsis at this stationary point, and to explain why there appears to be a barrier for the GeXY + CH$_4$ insertions. To our knowledge, this is the first theoretical study on the insertion of germylenes and the first application of DFT to the majority of these molecules. Thus, the present calculations can provide comprehensive energetic information on the insertion potential energy surface for all the reactions. Moreover, a better understanding of the thermodynamic and kinetic aspects of such insertions may help to optimize these and related syntheses.

II. Theoretical Methods

All geometries were fully optimized without imposing any symmetry constraints, although in some instances, the resulting structure showed various elements of symmetry. For our DFT calculations, we used the hybrid gradient-corrected exchange functional proposed by Becke,[25] combined with the gradient-corrected correlation functional of Lee, Yang, and Parr.[26] This functional is commonly known as B3LYP and has been shown to be quite reliable for geometries.[27] The standardized 6-311G basis set[28] was used together with polarization (*) functions.[28(b),29] We denote our B3LYP calculations by B3LYP/6-311G*. Vibrational frequency calculations at the B3LYP/6-311G* level were used to characterize all stationary points as either minima (the number of imaginary frequencies (NIMAG) = 0) or transition states (NIMAG = 1). All calculations were performed using the GAUSSIAN94/DFT package.[30]

(11) Karolczak, J.; Harper, W. W.; Grev, R. S.; Clouthier, D. J. *J. Chem. Phys.* **1995**, *103*, 2839.

(12) Bunker, P. R.; Phillips, R. A.; Buenker, R. J. *Chem. Phys. Lett.* **1984**, *110*, 351.

(13) Phillips, R. A.; Buenker, R. J.; Beardsworth, R.; Bunker, P. R.; Jensen, P.; Kraemer, W. P. *Chem. Phys. Lett.* **1985**, *118*, 60.

(14) Isabel, R. J.; Guillory, W. A. *J. Chem. Phys.* **1972**, *57*, 1116.

(15) Smith, G.; Guillory, W. A. *J. Chem. Phys.* **1972**, *56*, 1423.

(16) Harper, W. W.; Ferrall, E. A.; Hilliard, R. K.; Stogner, S. M.; Grev, R. S.; Clouthier, D. J. *J. Am. Chem. Soc.* **1997**, *119*, 8361.

(17) Takeo, H.; Curl, R. F.; Wilson, P. W. *J. Mol. Spectrosc.* **1971**, *38*, 464.

(18) Karolczak, J.; Grev, R. S.; Clouthier, D. J. *J. Chem. Phys.* **1994**, *101*, 891.

(19) Haruhiko, I.; Hirota, E.; Kuchitsu, K. *Chem. Phys. Lett.* **1990**, *175*, 384.

(20) Harper, W. W.; Clouthier, D. J. *J. Chem. Phys.* **1998**, *108*, 416.

(21) Hastie, J. W.; Hauge, R. H.; Margrave, J. L. *J. Mol. Spectrosc.* **1969**, *29*, 152.

(22) Karolczak, J.; Zhuo, Q.; Clouthier, D. J.; Davis, W. M.; Goddard, J. D. *J. Chem. Phys.* **1993**, *98*, 60.

(23) Haruhiko, I.; Hirota, E.; Kuchitsu, K. *Chem. Phys. Lett.* **1991**, *177*, 235.

(24) Coffin, J. M.; Hamilton, T. P.; Pulay, P.; Hargittai, I. *Inorg. Chem.* **1989**, *28*, 4092.

(25) (a) Becke, A. D. *Phys. Rev. A* **1988**, 38, 3098. (b) Lee, C.; Yang, W.; Parr, R. G. *Phys. Rev. B* **1988**, *37*, 785.

(26) Becke, A. D. *J. Chem. Phys.* **1993**, *98*, 5648.

(27) Su, M.-D.; Chu, S.-Y. Submitted.

(28) (a) For carbon, see: Krishnan, R.; Binkley, J. S.; Seeger, R.; Pople, J. A. *J. Chem. Phys.* **1980**, 72, 650. (b) For germanium, see: Curtiss, L. A.; McGrath, M. P.; Blaudeau, J.-P.; Davis, N. E.; Binning, R. C.; Radom, L. *J. Chem. Phys.* **1995**, *103*, 6104.

(29) Frisch, M. J.; Polpe, J. A.; Binkley, J. S. *J. Chem. Phys.* **1984**, *80*, 3265.
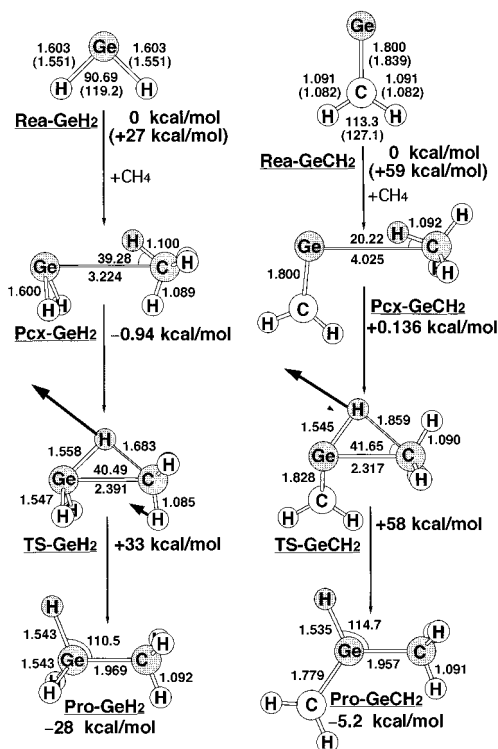
Figure 1. B3LYP/6-311G*-optimized geometries (in Å and deg) for the reactants (singlet and triplet), precursor complexes, transition states, and products of GeH$_2$ and Ge=CH$_2$. Values in parentheses are at the triplet state. The heavy arrows indicate the main atomic motions in the transition-state eigenvector.

III. Results and Discussion

A. Reactants. By analogy with all other known carbenes and silylenes, we expect that the two lowest states of germylene to be $^1A'$ and $^3A''$.[31] These states are derived from the ground-state HOMO, an essentially nonbonding σ orbital (A' symmetry) based on germanium, and the LUMO, an effectively nonbonding pπ orbital (A'' symmetry) on germanium. The optimized reactant geometries (**Rea**), i.e., GeH$_2$, Ge=CH$_2$, GeH(CH$_3$), Ge(CH$_3$)$_2$, GeHF, GeF$_2$, GeHCl, GeCl$_2$, GeHBr, and GeBr$_2$, for each reaction obtained at the B3LYP/6-311G* level of theory are collected in Figures 1−5. Tables 1 and 2 contain the structures, relative energies, and spectroscopic properties for the above molecules in the singlet ($^1A'$) and triplet ($^3A''$) states, together with some known experimental results.

The computed structures of the compounds GeH$_2$, GeF$_2$, GeCl$_2$, GeBr$_2$, GeHCl, and GeHBr are in good agreement with experiments, with the bond lengths and angles in agreement to within 0.04 Å and 1.0°, respectively (see Tables 1 and 2). As is usually the case in group 14 divalent compounds, the triplet state has significantly wider bond angles (∠XGeY) and shorter bond distances (Ge−X and Ge−Y) than the closed shell singlet state. In the case of GeX$_2$ (X = F, Cl, and Br), another trend that can be observed in Table 1 is the increase in the bond distances and bond angles for both $^1A'$ and $^3A''$ states as X

(30) Gaussian 94: M. J. Frisch, G. W. Trucks, H. B. Schlegel, P. M. W. Gill, B. G. Johnson, M. A. Robb, J. R. Cheeseman, T. Keith, G. A. Peterson, J. A. Montgomery, K. Raghavachari, M. A. Al-Laham, V. G. Zakrzewski, J. V. Ortiz, J. B. Foresman, J. Cioslowski, B. B. Stefanov, A. Nanayakara, M. Challacombe, C. Y. Peng, P. Y. Ayala, W. Chen, M. W. Wong, J. L. Andres, E. S. Replogle, R. Gomperts, R. L. Martin, D. J. Fox, J. S. Binkley, D. J. Defrees, J. Baker, J. P. Stewart, M. Head-Gordon, C. Gonzalez, and J. A. Pople. Gaussian, Inc., Pittsburgh, PA, 1995.

(31) For convenience, we used the C_s, rather than C_{2v}, symmetry throughout this work, even the molecule has no symmetry at all.
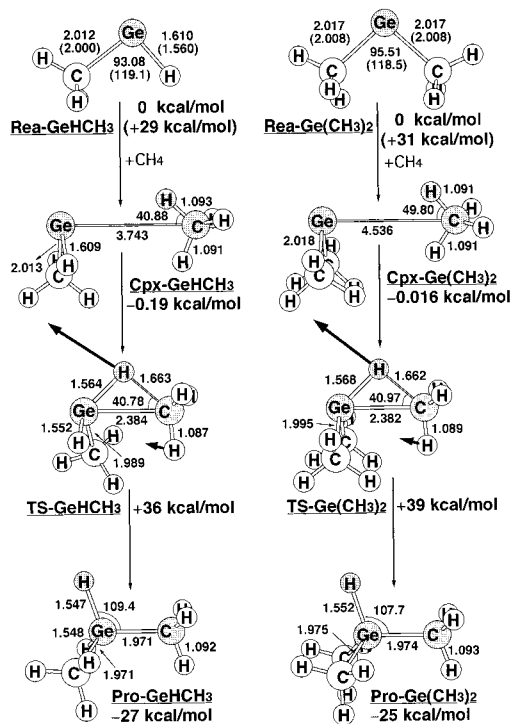
Figure 2. B3LYP/6-311G*-optimized geometries (in Å and deg) for for the reactants (singlet and triplet), precursor complexes, transition states, and products of GeHCH$_3$ and Ge(CH$_3$)$_2$. Values in parentheses are at the triplet state. The heavy arrows indicate the main atomic motions in the transition-state eigenvector.
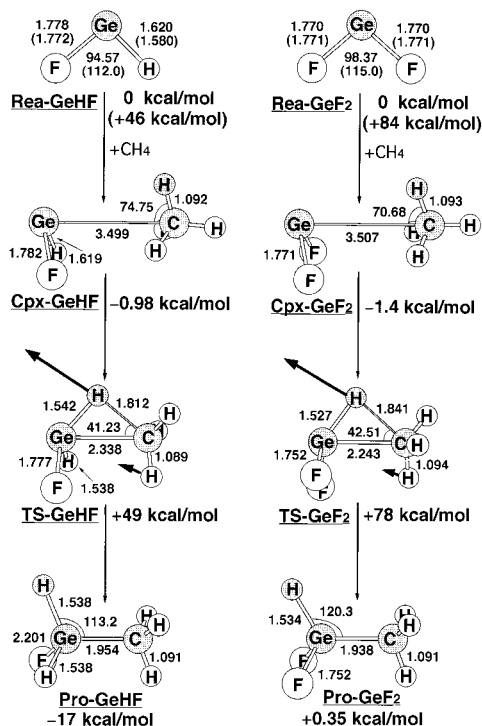
Figure 3. B3LYP/6-311G*-optimized geometries (in Å and deg) for the reactants (singlet and triplet), precursor complexes, transition states, and products of GeHF and GeF$_2$. Values in parentheses are at the triplet state. The heavy arrows indicate the main atomic motions in the transition-state eigenvector.

Figure 4. B3LYP/6-311G*-optimized geometries (in Å and deg) for the reactants (singlet and triplet), precursor complexes, transition states, and products of GeHCl and GeCl$_2$. Values in parentheses are at the triplet state. The heavy arrows indicate the main atomic motions in the transition-state eigenvector.

Figure 5. B3LYP/6-311G*-optimized geometries (in Å and deg) for the reactants (singlet and triplet), precursor complexes, transition states, and products of GeHBr and GeBr$_2$. Values in parentheses are at the triplet state. The heavy arrows indicate the main atomic motions in the transition-state eigenvector.

changes from F to Br. The increase in the bond angle can be explained as a consequence of the increase in the atomic radius from F to Br, which forces the bond to open up as one goes down the group. On the other hand, when going from GeH$_2$ to
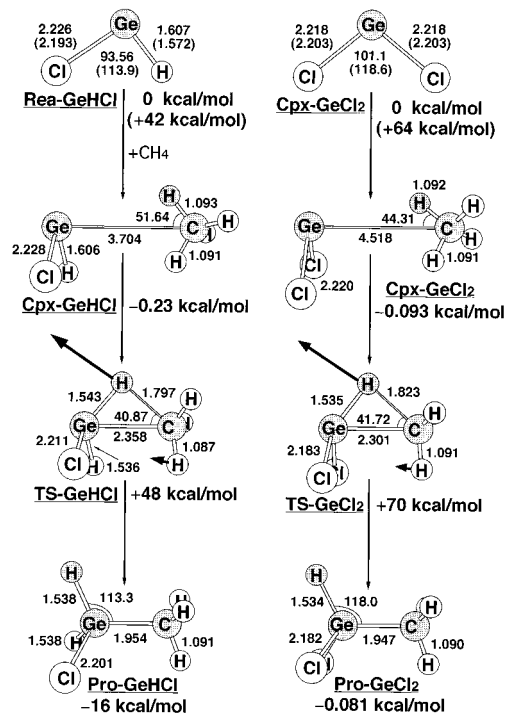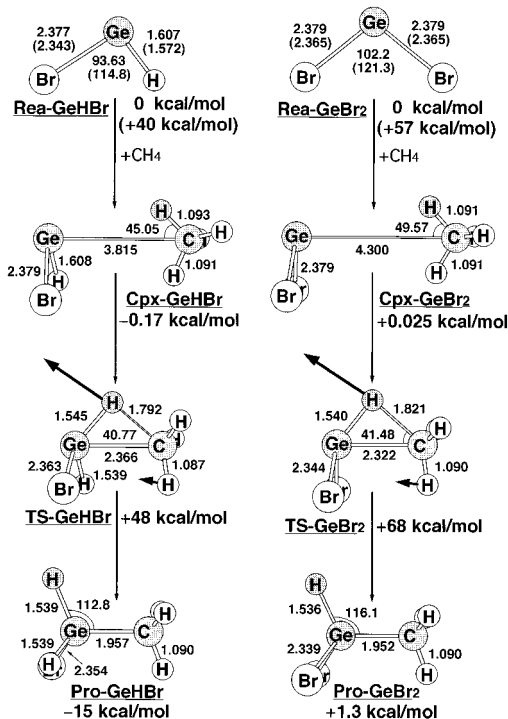
Ge(CH$_3$)$_2$, the bond angle increases for the ^{1}A′ singlet state and decreases for the ^{3}A″ triplet state (see Figures 1 and 2 and Table 1). Recently, the simplest unsaturated germylene, germylidene (Ge=CH$_2$), was characterized by Clouthier and collaborators.[16] Although no quantitative experimental results are available for

Table 1. Geometries, Relative Energies, and Spectroscopic Properties of GeX$_2$ (X = H, (CH$_3$), F, Cl, and Br) Obtained Using the B3LYP/6-311G* Level of Theory[a]

GeX$_2$	state	Ge−X (Å)	∠XGeX (deg)	ΔE_{rel}[b] (kcal/mol)	μ (D)	ν_1 (cm^{-1})	ν_2 (cm^{-1})	ν_3 (cm^{-1})
GeH$_2$	^{1}A′	1.603	90.69	0.0	0.2904	1869	958	1857
		[1.591]^c	[91.2]^c	(0.0)		[1887]^c	[920]^c	[1864]^c
GeH$_2$	^{3}A″	1.551	119.2	27.26	0.0564	2079	794	1988
				(1.182)				
Ge(CH$_3$)$_2$	^{1}A′	2.017	95.51	0.0	0.7787	526	211	516
				(0.0)				
Ge(CH$_3$)$_2$	^{3}A″	2.008	118.5	30.65	0.9126	550	155	494
				(1.329)				
GeF$_2$	^{1}A′	1.770	98.37	0.0	2.681	662	235	650
		[1.732]^d	[97.15]^d	(0.0)	[2.61]^d	[692]^d	[263]^d	[663]^c
GeF$_2$	^{3}A″	1.771	115.0	83.89	2.104	650	183	610
				(3.638)				
GeCl$_2$	^{1}A′	2.218	101.1	0.0	2.615	382	148	355
		[2.183]^e	[100.3]^e	(0.0)		[399]^e	[159]^e	[372]^c
GeCl$_2$	^{3}A″	2.203	118.6	63.66	1.394	382	105	336
				(2.760)				
GeBr$_2$	^{1}A′	2.379	102.2	0.0	2.209	276	98.3	266
		[2.377]^f	[101.2]^f	(0.0)		[286]^f	[110]^f	[276]^f
GeBr$_2$	^{3}A″	2.365	121.3	56.78	0.9045	282	71.0	224
				(2.462)				

[a] Values in square bracket denote the experimental data. [b] A positive value indicates a singlet ground state. Values in parentheses are in eV. [c] Reference 11. [d] Reference 18. [e] Reference22. [f] Reference 24.

Table 2. Geometries, Relative Energies, and Spectroscopic Properties of GeHX (X = (CH$_3$), F, Cl, and Br) Obtained Using the B3LYP/6-311G* Level of Theory[a]

GeHX	state	Ge−X (Å)	Ge−H (Å)	∠XGeH (deg)	ΔE_{rel}[b] (kcal/mol)	μ (D)	ν_1 (cm^{-1})	ν_2 (cm^{-1})	ν_3 (cm^{-1})
Ge=CH$_2$	^{1}A′	1.800^c	1.091^d	113.3^e	0.0	0.1899	791	424	683
					(0.0)				
Ge=CH$_2$	^{3}A″	1.839	1.082	127.1	59.03	0.2571	1250	749	851
					(2.560)				
GeH(CH$_3$)	^{1}A′	2.012	1.610	93.08	0.0	0.7028	889	532	603
					(0.0)				
GeH(CH$_3$)	^{3}A″	2.000	1.560	119.1	28.63	1.076	856	504	532
					(1.241)				
GeHF	^{1}A′	1.778	1.620	94.57	0.0	2.085	1795	647	754
					(0.0)				
GeHF	^{3}A″	1.772	1.580	112.0	46.43	2.190	1774	523	650
					(2.013)				
GeHCl	^{1}A′	2.226	1.607	93.56	0.0	2.345	1833	373	736
		[2.160]^f	[1.630]^f	[103]^f	(0.0)				
GeHCl	^{3}A″	2.193	1.572	113.9	42.16	1.906	1841	385	528
					(1.828)				
GeHBr	^{1}A′	2.377	1.607	93.63	0.0	2.038	1832	274	710
		[2.330]^f	[1.630]^f	[103]^f	(0.0)				
GeHBr	^{3}A″	2.343	1.572	114.8	40.40	1.417	1848	278	532
					(1.752)				

[a] Values in square bracket denote the experimental data. [b] A positive value indicates a singlet ground state. Values in parentheses are in ev. [c] The Ge=C bond length. [d] The C−H bond length. [e] The ∠HCH bond angle. [f] Reference 20.

both ^{1}A′ and ^{3}A″ states, its singlet ^{1}A′ structure based on the B3LYP/6-311G* level agrees well with that of the CISD calculations,[16] in which the bond lengths and angle are predicted to be 1.794 Å (Ge=C), 1.082 Å (C−H), and 114.2° (∠HCH).

We also calculated the dipole moments of all 10 species in their two lowest electronic states, which are given in Tables 1 and 2. It is worth pointing out that the calculated dipole moment of GeF$_2$, 2.681 D, is in good agreement with the experimental value of 2.61 D.[17] In addition, dipole moments of singlet and triplet states decrease as we go from GeF$_2$ to GeBr$_2$. This trend is reasonable if we consider the decrease in electronegativity from F to Br atoms. The GeF$_2$ molecule is expected to have the largest charge separation. However, the dipole moment also depends on the bond distance, and in this case, the GeBr$_2$ molecule possesses longer bonds than the GeF$_2$ and GeCl$_2$ molecules. In the case of GeHX (X = F, Cl, and Br), the bond distances, bond angles, and dipole moments (Table 2) follows a different trend to those of GeX$_2$. Presumably this is due to

the existence of weak interactions between the hydrogen and halogen atoms. This hydrogen bonding effect is also reflected in the fact that the bond angle of GeHX is smaller than that of GeX$_2$ in both singlet and triplet states.

The vibrational frequencies of all the germylenes studied in this work are presented in Tables 1 and 2. The theoretically predicted ground-state vibrational frequencies are generally in reasonable agreement with experimentally observed fundamental frequencies. For instance, the predicted ν_1 (symmetric stretches) are within 30 cm^{-1}, ν_3 (asymmetric stretches) within 17 cm^{-1}, and the low-frequency ν_3 (symmetric bends) within 38 cm^{-1} of their respective experimental values. Moreover, there are two related trends in the data which are of particular interest. As expected, the bond stretching (ν_1 and ν_3) and angle bending (ν_2) frequencies decrease along the series H, F, Cl, and Br. In addition, upon going from the ^{1}A′ singlet to the ^{3}A″ triplet, the loss of an electron from the HOMO causes the bond angle to widen in order to take more advantage of the bonding interac-

Table 3. HOMO and LUMO Energies (au) and Relative Energies (kcal/mol) for Singlet and Triplet GeXY Species and for the Process GeXY + H−CH$_3$ → Precursor Complex → Transition State → Product[a,b]

system	HOMO	LUMO	ΔE_{HO-LU}	ΔE_{st}[c]	reactants	ΔE_{cpx}[d]	$\Delta E^{\ddagger}$ [e]	ΔH[f]
GeH$_2$	−0.249	−0.123	0.126	+27.3	0	−0.936	+33.2	−28.0
Ge=CH$_2$	−0.221	−0.105	0.116	+59.0	0	−0.0487	+58.0	−5.25
GeHCH$_3$	−0.231	−0.106	0.125	+28.6	0	−0.191	+35.8	−26.8
Ge(CH$_3$)$_2$	−0.218	−0.0924	0.126	+30.7	0	−0.0157	+39.1	−25.1
GeHF	−0.260	−0.114	0.146	+46.4	0	−0.982	+48.6	−17.1
GeF$_2$	−0.321	−0.106	0.215	+83.9	0	−1.40	+77.7	+0.350
GeHCl	−0.263	−0.127	0.136	+42.2	0	−0.233	+48.1	−15.6
GeCl$_2$	−0.300	−0.131	0.169	+63.7	0	−0.0926	+70.0	−0.0812
GeHBr	−0.256	−0.127	0.130	+40.4	0	−0.171	+48.2	−14.5
GeBr$_2$	−0.282	−0.131	0.151	+56.8	0	+0.0247	+68.3	+1.28

[a] At the B3LYP/6-311G* level. [b] All optimized geometries can be found in Figures 1-5. [c] A positive value indicates a singlet ground state. [d] The stabilization energy of the precursor complex, relative to its corresponding reactants. [e] The activation energy of the transition state, relative to its corresponding reactants. [f] The reaction enthalpy of the product, relative to its corresponding reactants.

tions with the A′ orbital.[32] As a result, the wider angle has a smaller force constant, so the bending frequency decreases. In any event, the good agreement between experiment and theory on the known ground-state features gives us confidence in our theoretical predictions concerning the excited triplet states, where experimental data are less abundant.

This work, reliable when compared with available experimental data, shows that germylenes possess singlet ground states. Indeed, substituents more electronegative than Ge should result in a stabilization of the singlet state relative to the triplet state,[33] and so far, all germylenes generated experimentally have had singlet ground states. These trends run parallel to those observed and calculated for carbenes and silylenes,[33] but triplet ground states are not uncommon among carbenes.

Theoretical studies of GeH$_2$ have been performed by a number of groups with the most accurate calculations, giving a singlet−triplet separation of 22.8−23.6 kcal/mol.[34] The present calculations give 27.3 kcal/mol (27.5 kcal/mol after zero-point energy correction). In addition, it is intriguing to find that germylidene is also predicted to have a singlet ground state (see Table 2). The ^{1}A′−^{3}A″ energy gap is twice as large as that for GeH$_2$, 59.0 kcal/mol (59.7 kcal/mol after zero-point energy correction) at the B3LYP/6-311G* level. It should be mentioned here that the singlet−triplet energy gaps for those germylenes studied in this work may be overestimated by as much as several kilocalories per mole. Thus, using the more sphosticipated theory with larger basis sets is essential to obtain the most accurate results. Nevertheless, the energies obtained at the B3LYP/6-311G* level can, at least, allow reliable qualitative conclusions to be drawn.

Despite the fact that the ^{1}A′−^{3}A″ separation has not been measured experimentally, our DFT calculations provide several trends of interest. As can be seen from Tables 1 and 2, the most obvious trend is that strongly electron-withdrawing or π-donating substituents raise the singlet−triplet energy gap, whereas electropositive, π-accepting, or bulky substituents lower this energy gap. In addition, as is the case for the carbenes and silylenes, the halogen-substituted germylenes show a substantial stabilization of the singlet state over the triplet and thus higher separations are obtained. Namely, the stability of the singlet state of a halogermylene relative to the triplet increases as halogen electronegativity increases. For example, GeF$_2$ (84 kcal/mol) > GeCl$_2$ (64 kcal/mol) > GeBr$_2$ (57 kcal/mol) and GeHF (46 kcal/mol) > GeHCl (42 kcal/mol) > GeHBr (40 kcal/mol).

(32) Albright, T. A.; Burdett, J. K.; Whangbo, M.-H. In *Orbital Interactions in Chemistry*; John Wiley & Sons: New York, 1985.
(33) Harrison, J. F.; Liedtke, R. C.; Liebman, J. F. *J. Am. Chem. Soc.* **1979**, *101*, 7162.
(34) See ref 11 and references therein for recent work on GeH$_2$.

It should be noted that the effects of substituents on the singlet−triplet splitting are not additive. The increase in the singlet−triplet energy gap upon substitution of one H by CH$_3$ or F or Cl or Br is 1.4 or 19 or 15 or 13 kcal/mol; a second CH$_3$ or F or Cl or Br produces an additional increase by 2.0 or 37 or 21 or 16 kcal/mol, respectively. Therefore, each methyl group stabilizes the germylene singlet state preferentially by 1−2 kcal/mol, certainly a much smaller effect than halogen substitution. We shall use the above results to explain the origin of barrier heights for their insertion reactions in a latter section.

Finally, it should be noted that for all germylenes studied in this work the excitation energies from the singlet ground state to the first triplet excited state are quite large (ca. 27−84 kcal/mol). This means that the size of the singlet−triplet energy separation, in particular for the halogen-substituted germylenes, renders the production of the first excited triplet state under the experimental conditions practicably impossible. Thus, only the singlet potential surface was considered throughout this work.

B. Precursor Complexes. The geometries and energies of complexation of germylene with methane, i.e., **Pcx−GeH$_2$, Pcx−GeCH$_2$, Pcx−GeH(CH$_3$), Pcx−Ge(CH$_3$)$_2$, Pcx−GeHF, Pcx−GeF$_2$, Pcx−GeHCl, Pcx−GeCl$_2$, Pcx−GeHBr**, and **Pcx−GeBr$_2$** were also calculated. The optimized geometries are shown in Figures 1−5. For convenience, the energies are given relative to the two reactant molecules, i.e., GeXY + CH$_4$, which are also summarized in Table 3.

As seen in Figures 1−5, it is apparent that the precursor complexes all display very similar (XY)Ge- - -CH$_4$ bonding characteristics in which the GeXY unit is virtually orthogonal to the Ge−C axis. Calculated vibrational frequencies for the precursor complexes reveal that these structures are true minima on the potential energy surfaces. Compared to the structures of the isolated reactants, both germylene and methane geometries in those precursor complexes are essentially unperturbed. In addition, as one can see from Figures 1−5, the calculated bond distance for the Ge- - -C contacts (ca. 4.5−3.2 Å) are considerably longer than those calculated for the corresponding products (ca. roughly 1.9 Å; vide infra). Such long bond lengths are also reflected in the calculated complexation energies. As shown in Table 3, the energy of the precursor complex relative to its corresponding reactants is less than 1.4 kcal/mol. This strongly indicates that the intermediate germylene complex exists only as a shallow minimum and experimental detection of the intermediate formed during the reaction is unlikely.

C. Transition States. The optimized transition-state structures (**TS−GeH$_2$, TS−GeCH$_2$, TS−GeH(CH$_3$), TS−Ge(CH$_3$)$_2$, TS−GeHF, TS−GeF$_2$, TS−GeHCl, TS−GeCl$_2$, TS−GeHBr**, and **TS−GeBr$_2$**) along with the calculated transition vectors are

shown in Figures 1−5, respectively. The arrows in the figures indicate the directions in which the atoms move in the normal coordinate corresponding to the imaginary frequency. The geometries of all symmetrically substituted germylene GeX_2 shown in Figures are near C_s symmetry, although no symmetry restrictions were imposed in the transition searches.

Examination of the single imaginary frequency for each transition state (1164i cm^{-1} **TS−GeH$_2$**, 1118i cm^{-1} **TS−GeCH$_2$**, 1180i cm^{-1} **TS−GeH(CH$_3$)**, 1179i cm^{-1} **TS−Ge-(CH$_3$)$_2$**, 1137i cm^{-1} **TS−GeHF**, 1324i cm^{-1} **TS−GeF$_2$**, 1113i cm^{-1} **TS−GeHCl**, 1249i cm^{-1} **TS−GeCl$_2$**, 1111i cm^{-1} **TS−GeHBr**, and 1237i cm^{-1} **TS−GeBr$_2$**) provides excellent confirmation of the concept of the insertion process. The vibrational motion for the insertion of germylene into methane involves the bond forming between germanium and carbon in concert with C−H bond breaking and hydrogen transfer to the germanium center. Indeed, the primary similarity among all the transition states is the three-center pattern involving germanium, carbon, and hydrogen atoms.

A comparison of the 10 transition structures yields a number of trends. Increasing the number of halogens causes a larger decrease in the halogen-substituted germylene−CH$_4$ distance but leaves the methyl-substituted germylene−CH$_4$ distance relatively unaffected. That is, the newly forming Ge−C bond length decreases in the order: **TS−GeH$_2$** (2.391 Å) > **TS−GeHF** (2.338 Å) > **TS−GeF$_2$** (2.243 Å), **TS−GeHCl** (2.358 Å) > **TS−GeCl$_2$** (2.301 Å), and **TS−GeHBr** (2.366 Å) > **TS−GeBr$_2$** (2.322 Å), whereas **TS−GeH(CH$_3$)** (2.384 Å) ≈ **TS−Ge(CH$_3$)$_2$** (2.382 Å). In addition, the DFT calculations suggest that both the breaking C−H bond distance and the ∠GeCH bond angle increase in the order: **TS−GeH$_2$** (1.683 Å, 40.49°) < **TS−GeHF** (1.812 Å, 41.23°) < **TS−GeF$_2$** (1.841 Å, 42.51°), **TS−GeHCl** (1.797 Å, 40.87°) < **TS−GeCl$_2$** (1.823 Å, 41.72°), and **TS−GeHBr** (1.792 Å, 40.77°) < **TS−GeBr$_2$** (1.821 Å, 41.48°). All three features indicate that the transition structure occurs progressively later along the reaction path for insertion as the electronegative substitution is increased.

There is a dramatic effect on the internuclear distances at these saddle points. For GeH$_2$, GeH(CH$_3$), and Ge(CH$_3$)$_2$ insertions, the breaking C−H bonds are stretched by 54%, 52%, and 52%, respectively, relative to their values of methane (1.090 Å). In contrast, the analogous C−H bonds in Ge=CH$_2$, GeHF, GeF$_2$, GeHCl, GeCl$_2$, GeHBr, and GeBr$_2$ insertions are longer by 71%, 66%, 69%, 65%, 67%, 64%, and 67%, respectively, than the isolated methane. Taken together these features indicate that the transition structures for methyl-substituted germylenes take on more reactant-like character than halogen-substituted germylenes. Consequently, the barriers are encountered earlier in the reactions of the former than of the latter. As demonstrated below, this is consistent with the Hammond postulate[35] which associates an earlier transition state with a smaller barrier and a more exothermic reaction.

With halogen substitution, there is a large increase in the barrier height at the B3LYP/6-311G* level of theory. The first fluorine increases the barrier by ca. 49 kcal/mol and the second by an additional 29 kcal/mol. A similar increase in the barrier height is also found for chlorine and bromine substitutions (see Table 3). We also note that the barrier height for GeF$_2$ insertion (78 kcal/mol) is much higher than that for GeCl$_2$ insertion (70 kcal/mol), but this is not much higher than for the GeBr$_2$ one (68 kcal/mol). Highly electronegative groups such as F can lead to a substantially higher insertion barrier. Moreover, when comparing barrier heights of GeX$_2$ and of GeHX (X = halogen),

a greater difference appears along the series GeF$_2$ to GeBr$_2$ than along the series from GeHF (49 kcal/mol) to GeHCl (48 kcal/mol) to GeHBr (48 kcal/mol). In other words, the more the halogen substituents, the higher the activation energy.

Although germylidene is a short-lived germylene that is principally of theoretical interest, it is an excellent model to test any steric requirements for insertion since it has an empty 4p orbital that lies in the same plane as its trigonally hybridized adjacent methylene group. The B3LYP/6-311G* activation barrier (58 kcal/mol) for insertion into methane (**TS−GeCH$_2$**) is 25 kcal/mol higher than that for germylene insertion (**TS−GeH$_2$**), reflecting the destabilizing influence of the filled C−H σ orbitals on the adjacent methyl groups. It is worth noting that the magnitude of the activation barriers for methane insertion that we have examined so far depends more strongly on electronic factors than on steric interactions. For instance, the activation barriers for methyl and dimethyl germylene inserting into methane are 36 and 39 kcal/mol, but those for germylidene and halogen-substituted germylene insertion are in the range 48−78 kcal/mol.

D. Insertion Products. The optimized product geometries (**Pro−GeH$_2$**, **Pro−GeCH$_2$**, **Pro−GeH(CH$_3$)**, **Pro−Ge(CH$_3$)$_2$**, **Pro−GeHF**, **Pro−GeF$_2$**, **Pro−GeHCl**, **Pro−GeCl$_2$**, **Pro−GeHBr**, and **Pro−GeBr$_2$**) are collected in Figures 1−5. To simplify comparisons and to emphasize the trends, the calculated reaction enthalpies for insertion are also summarized in Table 3.

The theoretical results depicted in Figures 1−5 reveal that all the insertion products Ge(X)(Y)(H)(CH$_3$) adopt a staggered ethane-like structure. It should be noted that the newly formed Ge−C bonds in transition structures are stretched by an average 21% relative to their final equilibrium values in GeH$_2$, GeH-(CH$_3$), and Ge(CH$_3$)$_2$ insertions and 16%−19% for germylidene and halogen-substituted germylene insertions. Again, these features indicate that the methyl-substituted germylene insertion reaction reaches the TS relatively early, whereas the halogen-substituted germylene insertion arrives at the TS relatively late. Thus, one may anticipate a larger exothermicity for the former (see below).

Comparing the structures of the insertion product and its corresponding isolated reactants, as shown in Figures 1−5, it is interesting to note that the geometric parameters of the GeXY moiety in the products resemble more closely those of the triplet than those of the singlet GeXY reactants. This strongly implies that the triplet germylene should take part in the singlet surface during the insertion process. We shall explain this phenomenon in more detail in the next section.

The substituent effect on the heat of reaction is not additive. For instance, the present calculations predict that the reaction enthalpies of GeF$_2$, GeCl$_2$, and GeBr$_2$ insertions are 0.35, −0.081, and 1.3 kcal/mol, respectively. In contrast, our DFT results also suggest that the energies of **Pro−GeHF**, **Pro−GeHCl**, and **Pro−GeHBr** are below those of reactants by 17, 16, and 15 kcal/mol, respectively. On the other hand, as demonstrated in Table 3, the energetic ordering of the insertion of methyl-substituted germylene into CH$_4$ shows that the reaction enthalpy for the process is GeH$_2$ (−28 kcal/mol) < GeH(CH$_3$) (−27 kcal/mol) < Ge(CH$_3$)$_2$ (−25 kcal/mol) < Ge=CH$_2$ (−5.2 kcal/mol). Again, this is consistent with the observations shown earlier, in which the methyl-substituted germylene saddle point lies much closer to reactants than products.

E. Overview of Germylene Insertions. A schematic diagram of the GeXY + CH$_4$ (GeXY = GeH$_2$, Ge=CH$_2$, GeH(CH$_3$),

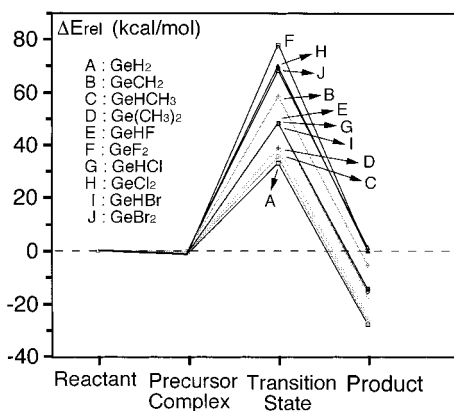(35) Hammond, G. S. *J. Am. Chem. Soc.* **1954**, *77*, 334.

Figure 6. Potential energy surfaces for the insertion of germylene into a C$-$H bond of CH_4. The relative energies are taken from the B3LYP/6-311G* level as given in Tables 1 and 2. The B3LYP-optimized structures of the stationary points see Figures 1$-$5.

$Ge(CH_3)_2$, GeHF, GeF_2, GeHCl, $GeCl_2$, GeHBr, and $GeBr_2$) potential surface is displayed in Figure 6.

The major conclusions that can be drawn from Figure 6 and Table 3 are as follows: (a) Considering both the activation barrier and exothermicity based on the model calculations presented here, we conclude that the methyl-substituted germylene insertions are much more favorable than those of the halogen-substituted germylenes. Indeed, from the magnitude of the insertion barriers, one can easily deduced that halogen-substituted germylenes should be relatively inert in the gas phase. (b) The more the halogen substituents, the higher the activation barrier and the less the exothermicity of a germylene insertion. This result can be also applied to the methyl-substituted germylenes. Nevertheless, the effect of methyl substitution is much smaller than halogen substitution. (c) Our theoretical findings suggest that C$-$H bonds are generally stable toward germylenes, which has been confirmed experimentally.[2] (d) Electronic factors, rather than steric factors, play a decisive role in determining the chemical reactivity of the germylene species from both a kinetic and thermodynamic viewpoint.

F. Comparison with Methylene and Silylene Insertions. Experiment[8] and theory[36] appear to be in agreement regarding the lack of a significant barrier in the $CH_2 + CH_4$ reaction. On the other hand, it has recently been demonstrated that the insertion of SiH_2 into a C$-$H bond of CH_4 occurs with a larger activation energy (17$-$19 kcal/mol).[37] Our DFT results suggest that the activation barrier for singlet GeH_2 insertion into methane is 33 kcal/mol.[38] This activation energy is considerably higher than for both CH_2 and SiH_2 insertions. Moreover, it has been shown that fluorine substitution leads to a large increase in the barrier height for carbene and silylene insertion into methane.[36] This is qualitatively consistent with our DFT results for the fluoro-substituted germylene insertions. In addition, the B3LYP calculations also suggest that the activation energies for GeF_2 and GeHF insertions are much higher than those for CF_2, CHF, SiF_2, and SiHF cases as shown previously.[36] A similar phenomenon can also be found in alkyl-substituted carbene[36] and germylene insertions. Although we have not carried out those calculations for the insertion of carbene and silylene into CH_4

(36) Bach, R. D.; Su, M.-D.; Aldabagh, E.; Andres, J. L.; Schlegel, H. B. *J. Am. Chem. Soc.* **1993**, *115*, 10237.

(37) (a) Sawrey, B. A.; O'Neal, H. E.; Ring, M. A.; Coffey, D. *Int. J. Chem. Kinet.* **1984**, *16*, 31. (b) Davidson, I. M. T.; Lawrence, F. T.; Ostah, N. A. *J. Chem. Soc., Chem. Commun.* **1980**, 659.

(38) However, the general trend of the B3LYP method to underestimate barrier heights is well-known, and it suggests that this B3LYP value is a lower limit.

using the same level of theory in this work, the fact that the activation barriers of germylenes are in general higher than those of carbenes and silylenes implies that the former should be much more inert than the latter during the insertion process.

IV. The Configuration Mixing Model

All of these computational results can be rationalized on the basis of a configuration mixing (CM) model based upon reactant and product spin recoupling.[39,40] In this approach, the reactant configuration and product configuration curves are used to create a reaction barrier. The former describes the electron distribution in the reactants, while the latter shows the electron distribution in the products.

The germylene insertion reaction (eq 1) may be described in valence bond (VB) terms by the avoided crossing of **1** and **2**. The VB configuration **1**, labeled ^{1}[GeXY]^1[CH$_4$], is termed the reactant configuration, in which the two electrons on the GeXY moiety are spin-paired to form the lone pair, while the two electrons on the CH_4 moiety are spin-paired to form a C$-$H σ bond. On the other hand, configuration **2** is the VB product configuration. Note that the spin arrangement is now different. The electron pairs are coupled to allow both Ge$-$C and Ge$-$H bond formation and simultaneous C$-$H bond breaking. To obtain this configuration from the reactant configuration **1**, each of the two original electron pairs needs to be uncoupled. In other words, those two electron pairs require excitation from the singlet state to the triplet state. Hence, this configuration is labeled ^{3}[GeXY]^3[CH$_4$]. It should be noted that ^{3}[GeXY]^3[CH$_4$] is an overall singlet configuration, despite the fact that it contains within it two local triplets. The MO representations of VB configurations **1** and **2** are shown in **3** and **4**, respectively. Consequently, it is the avoided crossing of these two configurations that leads to the simplest description of the ground-state energy profiles for the germylene insertion.
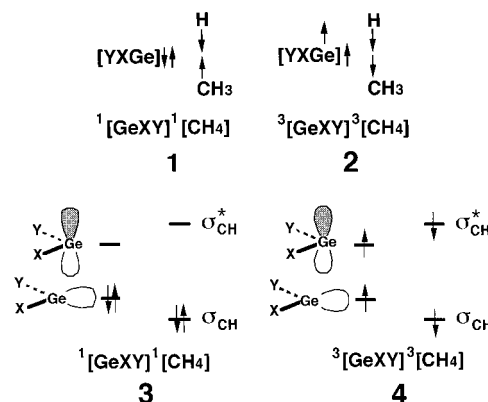
In Figure 7, we show the qualitative behavior of the two configurations for the insertion of germylene into CH_4. It is readily seen that the barrier height ($\Delta E^{\ddagger}$) as well as the reaction enthalpy (ΔH) may be expressed in terms of the initial energy gap between the reactant and product configurations. That is to say, the reactivity of germylene insertions will be governed by the singlet$-$triplet excitation energies for each of the reactants, i.e., ΔE_{st} ($= E_{triplet} - E_{singlet}$ for GeXY) and $\Delta E_{\sigma\sigma*}$ ($= E_{triplet} - E_{singlet}$ for CH_4). Accordingly, if $\Delta E_{\sigma\sigma*}$ is a constant, then a smaller value of ΔE_{st} leads to (i) reduction of the reaction barrier

(39) (a) Shaik, S.; Schlegel, H. B.; Wolfe, S. In *Theoretical Aspects of Physical Organic Chemistry*; John Wiley & Sons Inc.: New York, 1992. (b) Pross, A. In *Theoretical and Physical principles of Organic Reactivity*; John Wiley & Sons Inc.: New York, 1995.

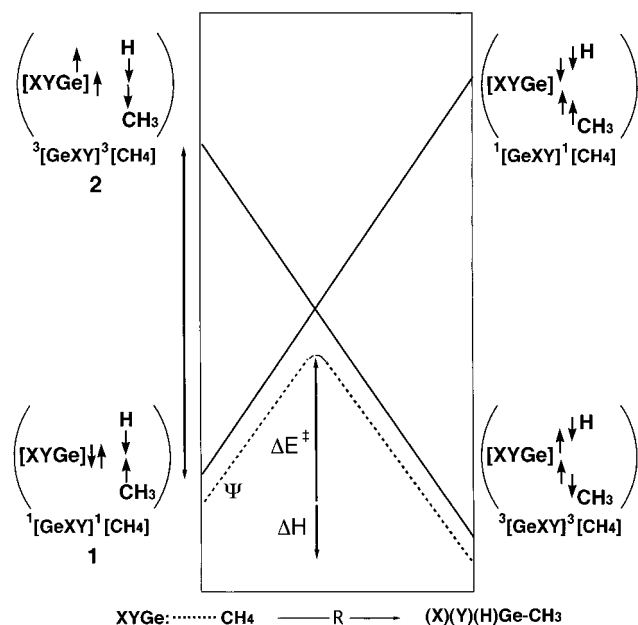(40) Su, M.-D. *Inorg. Chem.* **1995**, *34*, 3829.

Figure 7. Energy diagram for an insertion reaction showing the formation of a state curve (Ψ) by mixing two configurations: the reactant configuration (1) and the product configuration (2). It can be seen that both the activation energy ($\Delta E^{\ddagger}$) and reaction enthalpy (ΔH) is proportional to ΔE_{st} (=$E_{triplet} - E_{singlet}$ for GeXY) and $\Delta E_{\sigma\sigma^*}$ (=$E_{triplet} - E_{singlet}$ for CH$_4$). See the text.
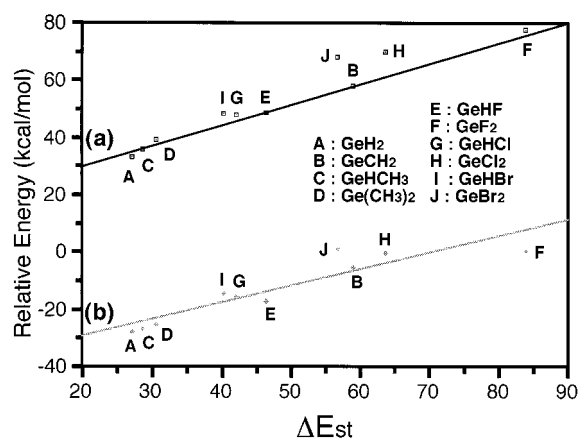
Figure 8. ΔE_{st} (=$E_{triplet} - E_{singlet}$) for germylene GeXY vs the activation energy and reaction enthalpy for the insertion of GeXY into H$-$CH$_3$. The linear regression equation is (a) $\Delta E^{\ddagger} = 0.818\Delta E_{st} + 13.5$ and (b) $\Delta H = 0.584\Delta E_{st} - 41.1$ with a correlation coefficient $R = 0.93$ and $R = 0.94$, respectively. All values were calculated at the B3LYP/6-311G* level. See the text.

since the intended crossing of ^{1}[GeXY]^1[CH$_4$] and ^{3}[GeXY]-^{3}[CH$_4$] is lower in energy and (ii) a larger exothermicity since the energy of the product is now lower than that of the reactant. In short, the smaller the ΔE_{st} of GeXY, the lower the barrier height, and in turn, the faster the insertion reaction, the larger the exothermicity.

Our model calculations confirm the above prediction. For the B3LYP/6-311G* calculations on the 10 systems studied here, a plot of activation barrier versus ΔE_{st} is given in Figure 8: the best fit is $\Delta E^{\ddagger} = 0.818\Delta E_{st} + 13.5$. Likewise, the linear correlation between ΔE_{st} and the reaction enthalpy (ΔH), also obtained at the same level of theory, is $\Delta H = 0.584\Delta E_{st} - 41.1$. This investigation provides strong evidence that the singlet$-$triplet energy gap can be used as a guide to predict the reactivity of germylenes. Thus, to find a good model for facile insertion reactions, an understanding of the singlet$-$triplet

splitting ΔE_{st} of germylene is crucial. Furthermore, we have also examined the relationship between the HOMO$-$LUMO energy gaps and the activation barriers for the aforementioned 10 systems as shown in Table 3. Our theoretical findings suggest that neither HOMO and LUMO energies nor HOMO$-$LUMO energy gaps correlate well with the increase in the insertion barriers. This is not surprising since the singlet$-$triplet excitation energy is the HOMO$-$LUMO energy difference minus the orbital Coulombic repulsion integral.[41] In other words, the singlet$-$triplet splitting ΔE_{st} is not equivalent to the HOMO$-$LUMO energy gap, so that the latter is not directly associated with the activation energy for insertion.

Before further discussion, let us emphasize here the importance of the status of the triplet germylene GeXY. Since two new covalent bonds have to be formed in the product GeXY-(H)(CH$_3$), i.e., the Ge$-$C and Ge$-$H bonds (right in Figure 7), the bond-prepared GeXY state must have at least two open shells, and the lowest state of this type is the triplet state. Therefore, from the valence-bond point of view, the bonding in the product can be recognized as bonds formed between the triplet GeXY state and the two doublet radicals (overall singlet), the methyl radical and the hydrogen atom. This is similar to considering the bonds in a water molecule as being formed between a triplet oxygen atom and two doublet hydrogen atoms.[42] Therefore, if a reactant GeXY has a singlet ground state with a low-lying triplet state, it will readily undergo single-step bond insertions due to involvement of the triplet state in the reaction. The supporting evidence comes from the fact that geometrical parameters of the final product resemble those of the corresponding triplet reactants. This is exactly what we have seen in our DFT results as shown earlier.

The effect of replacing carbon (carbenes) with germanium (germylenes) without altering substituents is predicted to result in a stabilization of the singlet relative to the triplet. As often observed in carbene and silylene, ΔE_{st} of germylenes increases as the electronegativity of the substituents is increased. This is due to the fact that π-donor substituents favor the singlet state by bonding with the p-orbital on the germanium, which is vacant in the singlet state and singly occupied in the triplet.[43] Moreover, as discussed earlier, singlet germylenes have smaller bond angles than triplets and, therefore, have more germanium p-character in the bonds to the substituents. The greater p-character leads to stronger ionic bonding and stabilization of the singlet. This stabilization is naturally more important for more electronegative substituents, resulting in an increase in ΔE_{st} with substituent electronegativity.[33] In fact, the alternative explanations of π-donation and electron-withdrawal are readily compatible. Electronegative substituents withdraw electron density from the germanium, making it more positively charged. This increased positive charge makes the germanium a better π-acceptor. As a result, π-donation from substituents is enhanced.[44]

Conversely, sterically bulky substituents favor a large $\angle$XGeY bond angle, leading to more germanium s character in the Ge$-$X bonds and therefore more p-character in the germanium non-bonding σ-orbital. This reduce the energy difference between the nonbonding valence s- and p-orbitals, favoring the triplet state and thereby reducing the singlet$-$triplet splitting. At the other extreme, an electropositive substituent (with respect to germanium) will, in the limit, result in an in situ Ge^{2-} which,

(41) See ref 32, pp 116.
(42) Siegbahn, P. E. M. *J. Am. Chem. Soc.* **1996**, *118*, 1487.
(43) Irikura, K. K.; Goddard, W. A., III; Beauchamp, J. L. *J. Am. Chem. Soc.* **1992**, *114*, 48.
(44) Such π-back-bonding is commonplace in transition metal chemistry, although the ligands are usually the σ-donors and π-acceptors in that context.

being isoelectronic with ^3P oxygen, will favor a triplet state. Again, this will reduce the singlet−triplet separation or even yield a triplet ground state. In any event, strongly electron-withdrawing or π-donating substituents will raise the singlet−triplet energy gap, while electropositive or bulky substituents will lower this energy gap.

In summary, from the analysis in the present study, we are confident in predicting that, for the substituted germylenes GeXY, the more strongly π-accepting, the bulkier, or the more electropositive the substituents, the smaller the ΔE_{st} of GeXY, the lower the activation energy, and the larger the exothermicity for the insertion of germylenes into saturated C−H bonds.[45] In contrast, electronegative or π-donating substituents will result in a larger ΔE_{st}. These species will tend not to undergo insertion reactions.

Despite the fact that the estimated magnitude of the barrier for such insertions and the predicted properties of the germylene species appear to be dependent on the level of calculation applied, our qualitative predictions are in accord with the theoretical results presented here as well as the available experimental observations. Despite the simplicity, our approach can provide chemists with important insights into the factors controlling the activation of saturated bonds and thus permit them to predict the reactivity of several, as yet unknown, reactive GeXY intermediates.

It is hoped that our study will stimulate further research into the subject.

(45) Su, M.-D.; Chu, S.-Y. Submitted.